SLAC-PUB-2340
May 1979
(M)

FIRST RESULTS FROM MARK II AT SPEAR*,**

G. S. Abrams, M. S. Alam, C. A. Blocker, A. M. Boyarski, M. Breidenbach, C. H. Broll, D. L. Burke, W. C. Carithers, W. Chinowsky, M. W. Coles, S. Cooper, B. Couchman, W. E. Dieterle, J. B. Dillon, J. Dorenbosch, J. M. Dorfan, M. W. Eaton, G. J. Feldman, H. G. Fischer, M.E.B. Franklin, G. Gidal, G. Goldhaber, G. Hanson, K. G. Hayes, T. Himel, D. G. Hitlin, R. J. Hollebeek, W. R. Innes, J. A. Jaros, P. Jenni, A. D. Johnson, J. A. Kadyk, A. J. Lankford, R. R. Larsen, M. J. Longo, D. Lüke, V. Lüth, J. F. Martin, R. E. Millikan, M. E. Nelson, C. Y. Pang, J. F. Patrick, M. L. Perl, B. Richter, J. J. Russell, D. L. Scharre, R. H. Schindler, R. F. Schwitters, S. R. Shannon, J. L. Siegrist, J. Strait, H. Taureg, V. I. Telnov, M. Tonutti, G. H. Trilling, E. N. Vella, R. A. Vidal, I. Videau J. M. Weiss, H. Zaccone.

Presented by Peter Jenni.†

†Stanford Linear Accelerator Center
Stanford University, Stanford, California 94305
and
Lawrence Berkeley Laboratory and Department of Physics
University of California, Berkeley, California 94720

ABSTRACT

First results from the SLAC-LBL Mark II magnetic detector at SPEAR are presented. The performance of the detector is discussed and preliminary results are given on inclusive baryon production $R_{p+\bar{p}}$, $R_{\Lambda+\bar{\Lambda}}$, on decay modes of the D mesons and on two-photon production of η' mesons.

*This work was supported primarily by the Department of Energy under contract numbers DE-AC-03-76SF00515 and W-7405-ENG-48.

**Invited talk at the Highly Specialized Seminars, 5th Session: Probing Hadrons with Leptons, "Ettore Majorana" Centre for Scientific Culture, Erice, Sicily, Italy, March 13-21, 1979.

I. INTRODUCTION

In this talk I will report some of the first results from the Mark II experiment at the Stanford Linear Accelerator Center e^+e^- storage ring facility SPEAR. The first part will be devoted to a description of the Mark II detector and of its performance. Then I will show preliminary results on a measurement of the inclusive production of baryons (p, $\bar{p}$, Λ and $\bar{\Lambda}$) over the center of mass energy range from 4.5 to 6 GeV in a search for a threshold of charmed baryon production. Data on decays of charmed D mesons have been accumulated at the ψ'' (3770) resonance and first results will be given in part three from an analysis of about one third of the whole data sample. Finally, we have observed for the first time evidence for η' (958) production in two-photon collisions. We measured the radiative width of the η' through this process as will be discussed in the last part of this talk.

II. THE MARK II DETECTOR

A schematic view of the Mark II detector is shown in Fig. 1. A particle that moves outwards from the e^+e^- interaction region first traverses the 0.15 mm thick stainless steel vacuum pipe and two concentric 0.64 cm thick cylindrical scintillation counters. It then enters the drift chamber[1] which contains 16 sense-wire layers of radii 0.41 m to 1.45 m. The wire orientation is such as to provide the highest accuracy in the transverse direction: 6 of the

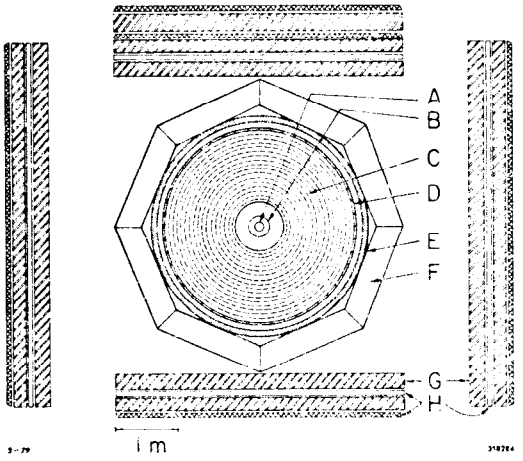

Fig. 1. Schematic view of the Mark II detector. (A) vacuum chamber, (B) pipe counter, (C) drift chamber, (D) time-of-flight counters, (E) solenoid coil, (F) liquid argon shower counters, (G) iron absorber, (H) muon proportional tubes.

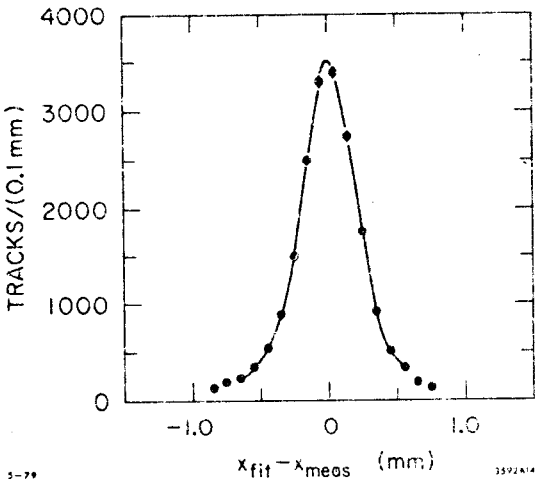

Fig. 2. Example of a distribution of the difference between fitted and measured track positions in the drift chamber.

layers have wires parallel to the beam axis and the other 10 are at a small stereo angle ($\pm 3^{o}$) with respect to the beam axis. The average spacial resolution is about 210 μm per layer. Figure 2 shows an example of a distribution of the difference between fitted and measured track positions. The magnetic field is 4.1 kG and the momenta of charged particles are measured with an accuracy $\delta p/p = \pm[(0.010p)^2 + (0.0145)^2]^{\frac{1}{2}}$ where p is the momentum in GeV/c.*

The drift chamber is surrounded by a layer of 2.54 cm thick scintillation counters. Each counter is viewed on both ends by XP2230 photomultipliers. With the beam crossing reference signal they provide an rms time-of-flight resolution of 300 ps for hadrons and 270 ps for Bhabha scattered electrons (Figure 3).

Next, the particle traverses 1.36 radiation-lengths of solenoidal coil and support material and enters one of the eight liquid argon calorimeter modules[2] (LA). A module consists of a "massless" trigger gap with 0.16 cm thick Al electrodes and two 0.8 cm thick liquid argon gaps followed by 18 sampling layers with 0.2 cm thick Pb ground planes alternating with 3.7 cm wide, 0.2 cm thick Pb read-out strips and 0.3 cm liquid argon gaps. These shower counters are about 14 radiation lengths deep. The read-out strips are parallel, perpendicular and at 45^{o} to the beam axis giving an rms angular resolution of about 8 mrad both in azimuth and dip angle. The rms energy resolution for electrons and photons at high energies ($\geq$ 0.5 GeV) has been measured to be $\delta E/E = 0.11/\sqrt{E}$ (E in GeV). An example for Bhabha scattered electrons at the beam energy

*The momentum resolution is $\delta p/p = \pm[(0.005p)^2 + (0.0145)^2]^{\frac{1}{2}}$ when tracks are constrained to pass through the known beam position.

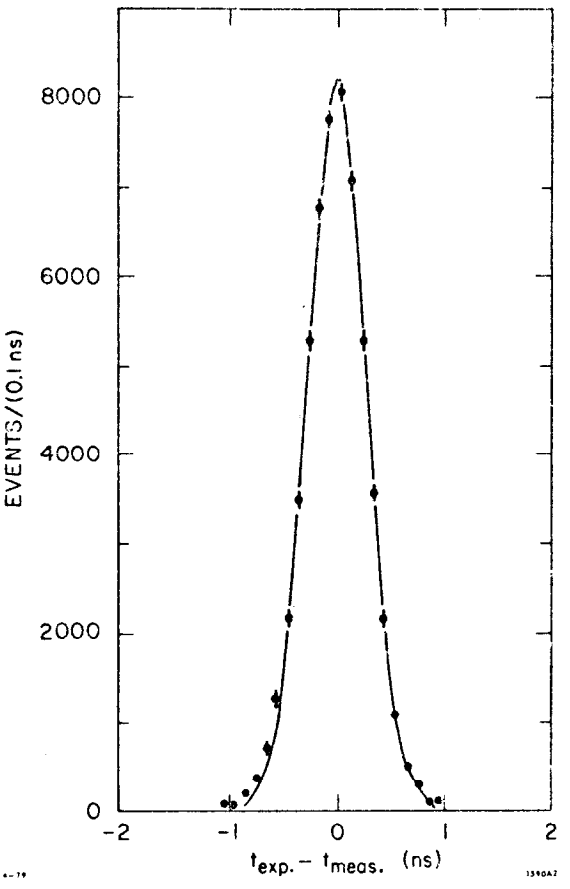

Fig. 3. Expected time minus measured time from the TOF system for a sample of Bhabha events at $E_{CM} = 4.16$ GeV.

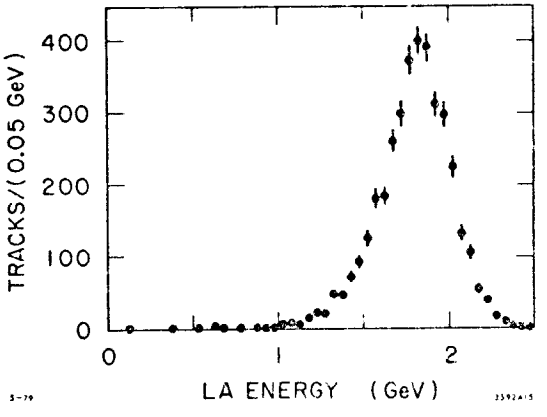

Fig. 4. Energy distribution in the liquid argon calorimeter modules for a sample of Bhabha scattered electrons at $E_{CM} = 3.684$ GeV.

E = 1.842 GeV is shown in Figure 4. At lower energies the resolution is worse ($0.13/\sqrt{E}$) because of the increasing importance of the energy loss in the coil material. The measured efficiency for photons within the geometrical acceptance of the LA detector is shown in Figure 5 and agrees well with detailed electromagnetic shower Monte Carlo calculations[3] (shown as curve in Figure 5) which are also used to correct the measurements for the energy loss in the coil material. The LA detector is also used for electron-pion separation. Pion misidentification probabilities of less than 5% for electron efficiencies above 75% are achieved for particle momenta greater than 500 MeV/c, and improve with higher momenta. Finally two 23 cm thick steel walls each followed by one plane of proportional tubes are used for the detection of muons above $p \approx 700$ MeV/c.

The fraction of the full solid angle covered by the drift chamber and TOF counters is about 75%, by the LA modules is 70%, and by the muon detection system is 55%. At small angles relative to the beams there are additional shower counters (at one end a liquid argon calorimeter and at the other end two planes of proportional chambers each preceded by 1.1 cm of lead) which extend the solid angle coverage to 90% of 4π sr.

The detector is triggered with a two stage hardware trigger[4] that selects with efficiency ≥99% all interactions that emit at least one charged particle through the entire drift chamber and another particle through at least its first 5 layers. The luminosity is measured with independent shower counters detecting Bhabha scattering at 22 mrad and checked against wide angle Bhabha events observed in the detector. The systematic uncertainty in the luminosity is less than ±6%.

In Figure 6 we show a (particularly high multiplicity) example of a multiprong hadron event at $E_{CM} = 5.08$ GeV as reproduced by the online event display. The event is shown in the projection into a

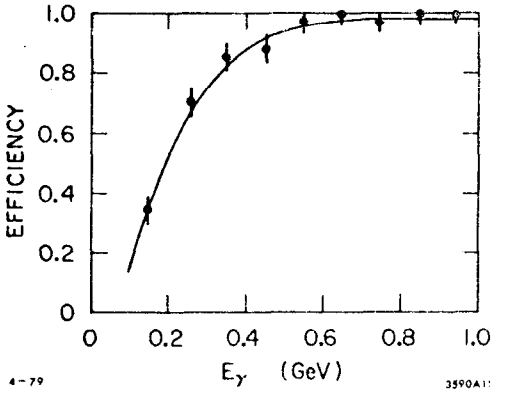

Fig. 5. Detection efficiency for photons within the geometrical acceptance of the LA barrel modules. The curve is a Monte Carlo calculation.

plane perpendicular to the beam axis displaying the track measurements in the drift chamber, the time-of-flight counters and the liquid argon shower counters (with the corresponding energies in GeV).

III. INCLUSIVE BARYON PRODUCTION

The inclusive production of baryons has been studied in a scan over the center of mass energy range from 4.5 to 6 GeV. At this early stage of the analysis we present results for $\bar{p}$, Λ and $\bar{\Lambda}$ production, also including data from running at various fixed energies. The p and $\bar{p}$ identification has been done by the time-of-flight measurement. The Λ ($\bar{\Lambda}$) have been observed by their $p\pi^-$ ($\bar{p}\,\pi^+$) decay mode with a rms mass resolution of about 3 MeV/c^2.

The results, corrected for the acceptance, are given in Figure 7 as the ratio of the inclusive cross section to the μ-pair production cross section. To avoid beam-gas backgrounds, only the $\bar{p}$ measurements have been used in the case of Figure 7(a); plotted is $R(\bar{p}+p) = 2\sigma_{\bar{p}}/\sigma_{\mu\mu}$. All the errors shown are only statistical;

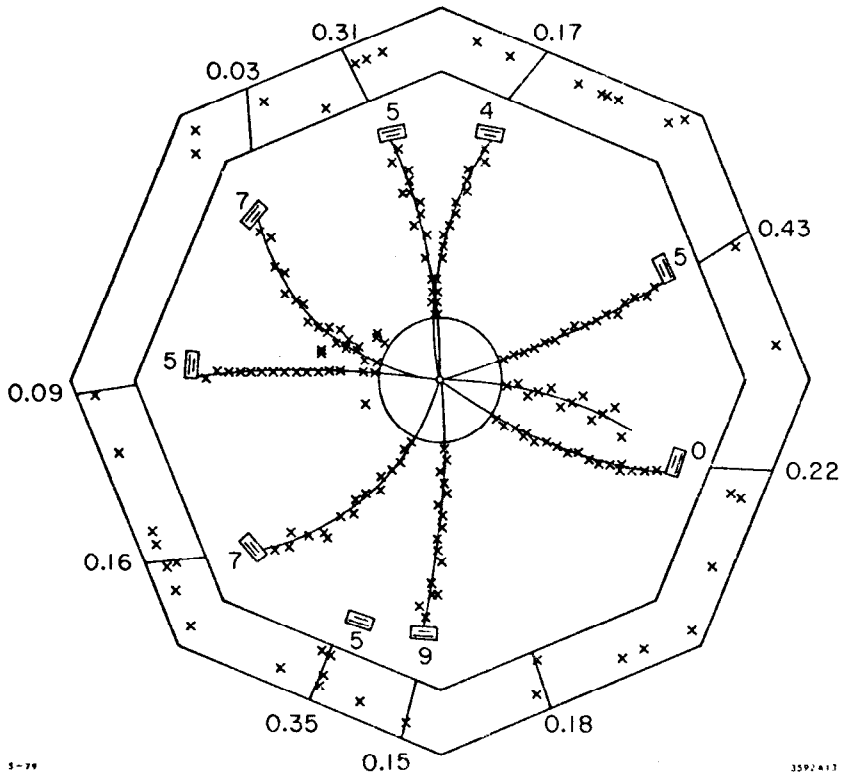

Fig. 6. Example of a (particularly high multiplicity) multiprong hadron event at $E_{CM} = 5.08$ GeV as produced by the online event display. (See text.)

the systematic uncertainty of $R(\bar{p} + p)$ and $R(\bar{\Lambda} + \Lambda)$ is estimated to be less than ±20%. The measurements are consistent with previous experiments[5,6] and confirm in more detail the rise in the inclusive baryon production in e^+e^- annihilation over the center of mass energy range of about 4.5 to 5.5 GeV.

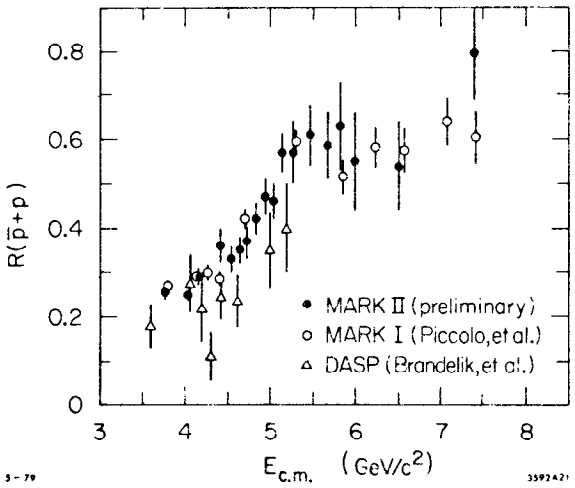

Figure 7(a)

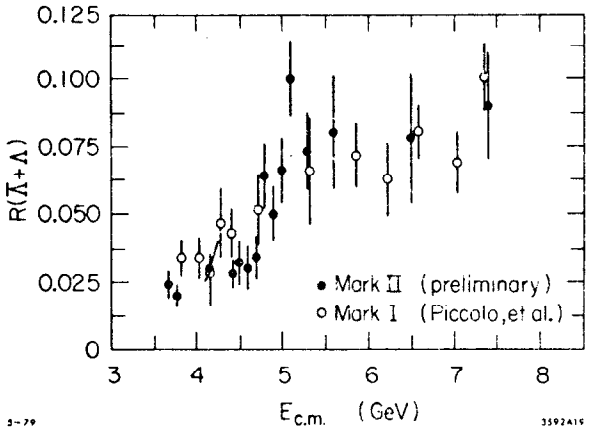

Figure 7(b)

Fig. 7. Inclusive $\bar{p}$ and $\Lambda + \bar{\Lambda}$ production. (a) $R(\bar{p} + p) = 2\sigma(\bar{p})/\sigma_{\mu\mu}$ vs. c.m. energy. (b) $R(\bar{\Lambda} + \Lambda) = \sigma(\bar{\Lambda} + \Lambda)/\sigma_{\mu\mu}$ vs. c.m. energy. The Mark II results are preliminary, the systematic uncertainty for these measurements is estimated to be less than ±20%. [Mark I is Reference (5); DASP is reference (6)].

IV. CHARMED D MESON DECAYS

Various decay modes of the charmed D mesons are being studied with the data that have been accumulated at the ψ'' (3770) resonance.[7] The first results reported here are based on a total integrated luminosity of 770 nb^{-1} which represents slightly more than one quarter of the total data sample.

The charged particle identification has been done by the time-of-flight and liquid argon pulse height measurements and π^0's have been reconstructed in the liquid argon shower detectors. The total energy of a reconstructed D meson has been constrained to the known beam energy (because of ψ'' (3770) $\rightarrow D\bar{D}$).

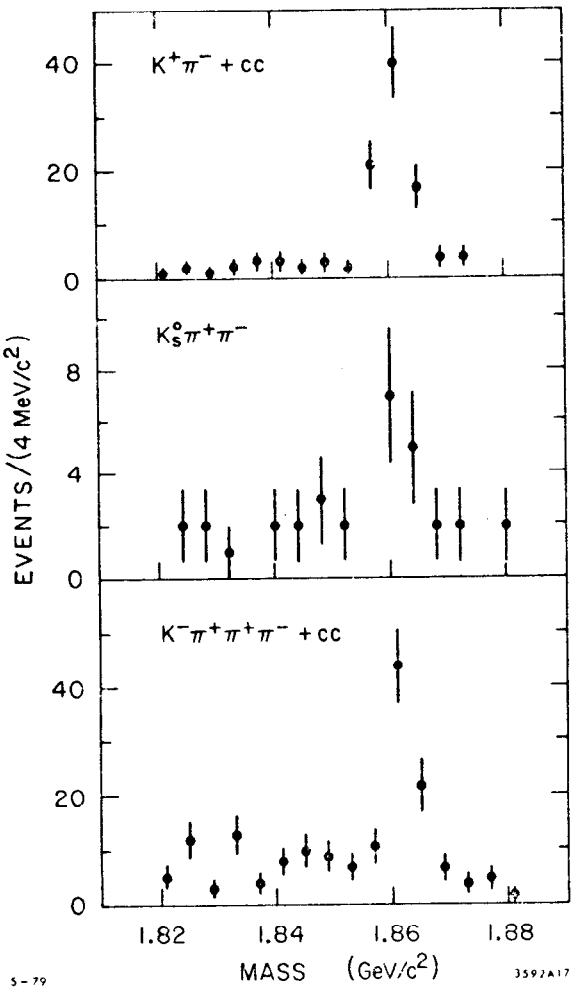

Fig. 8. Invariant mass distribution for various D^0 decay modes.

A further constraint is possible in the D decays involving π^0 or K_S^0 where the observed $\gamma\gamma$ or $\pi^+\pi^-$ final states have been fit to the known mass values respectively. The rms mass resolution achieved on the reconstructed D mesons is typically 2 - 3 MeV/c^2. Invariant mass distributions for different observed decay modes of the D^0, $\bar{D}^0$ and $D^\pm$ are shown in Figures 8 and 9. In Table 1 we summarize the branching ratios which have been obtained in this preliminary analysis. The errors given do include the uncertainty in the total cross section measurement of the ψ'' (3770) resonance measured in a previous experiment.[8] However, a further estimated systematic uncertainty of ±20% is not included. All values are in good agreement with the previous measurements of the Mark I collaboration.[3,9]

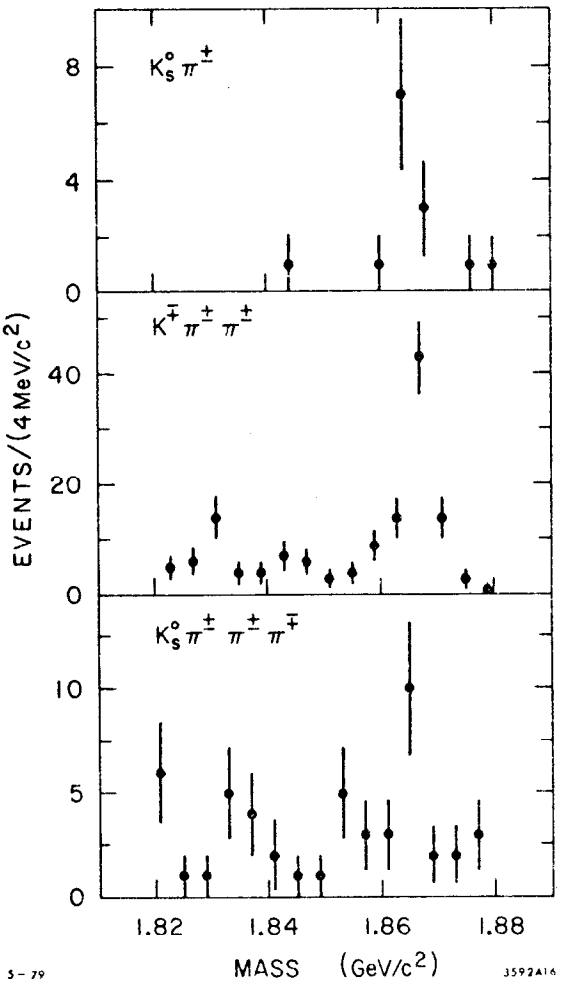

Fig. 9. Invariant mass distribution for various $D^\pm$ decay modes.

Table 1. Preliminary Measurement of Various Branching Ratios of D mesons.

Decay Mode	Detection Efficiency	Number of Events	Branching Ratio
$D^0 \to K^{\pm}\pi^{\mp}$	0.44	74 ± 10	0.019 ± 0.005
$K^{\pm}\pi^{\mp}\pi^{\mp}\pi^{\pm}$	0.10	55 ± 10	0.061 ± 0.019
$K^{\pm}\pi^{\mp}\pi^{0}$	0.024	18 ± 5	0.083 ± 0.022
$K^{0}_{S}\pi^{+}\pi^{-}$	0.13	12 ± 4	0.010 ± 0.004
$D^{\pm} \to K^{\mp}\pi^{\pm}\pi^{\pm}$	0.29	65 ± 9	0.032 ± 0.008
$K^{0}_{S}\pi^{\pm}$	0.24	10 ± 3	0.005 ± 0.003
$K^{0}_{S}\pi^{\pm}\pi^{\pm}\pi^{\mp}$	0.04	12 ± 5	0.040 ± 0.023

V. EVIDENCE FOR η' (958) PRODUCTION IN TWO-PHOTON COLLISIONS

The observation of leptons and hadrons produced by two-photon interactions in electron-positron colliding beam experiments has been a challenge ever since the importance of the two-photon mechanism has been pointed out.[10] The basic diagram is shown in Figure 10. Lepton pairs produced by the two-photon process have been observed in several experiments.[11,12] The data on hadronic events are much more scarce as only a very few multi-hadron events have been seen[13] so far.

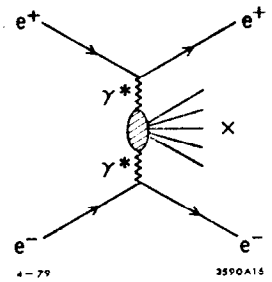

Fig. 10. Diagram for the two-photon production of the state X.

We have observed and reported[14] evidence for η' (958) production in the reaction

$$e^+e^- \rightarrow e^+e^-\eta' \qquad (1)$$

through the decay mode $\eta' \rightarrow \rho^0\gamma$ resulting in a $\pi^+\pi^-\gamma$ final state. The outgoing e^+ and e^- were not detected.

Events having only two oppositely charged tracks coming from the interaction region and one photon detected in the LA modules were selected. The pions were identified by TOF measurement and by LA pulse heights (to eliminate electrons). A few kinematical cuts were applied to reduce possible backgrounds from one photon e^+e^- annihilations, where part of the final state particles remain undetected, from Bhabha scattered electrons with radiatively degraded initial states, and from lepton or pion pairs produced in two-photon interactions combined with noise-generated false photons. All the analysis cuts are listed in Reference (14); the two most important ones are requiring that the transverse momentum of the $\pi^+\pi^-\gamma$ state ($p_\perp$) be <250 MeV/c and that the acoplanarity angle between the $\pi^+\pi^-$ pair and the γ momentum vectors defined with respect to the beam axis ($\Delta\phi$) be <0.5 rad ($\Delta\phi = 0$ for back-to-back decays).

The $\pi\ \pi\ \gamma$ mass distribution for the remaining events, given in Figure 11, shows a clear $\eta' \rightarrow \pi^+\pi^-\gamma$ signal. The η' mass resolution is dominated by the photon energy measurement and is consistent with the expectation.

The transverse momentum $p_\perp$, total energy E and angular distribution cos θ (with respect to the beam axis) are shown in Figures 12a-c for all events (full histogrammes) and for the events lying in the η' mass region (shaded) defined as $800 < m_{\pi\pi\gamma} < 1100$ MeV/c^2. The η' events occur mainly at low $p_\perp$ in contrast with the background events.

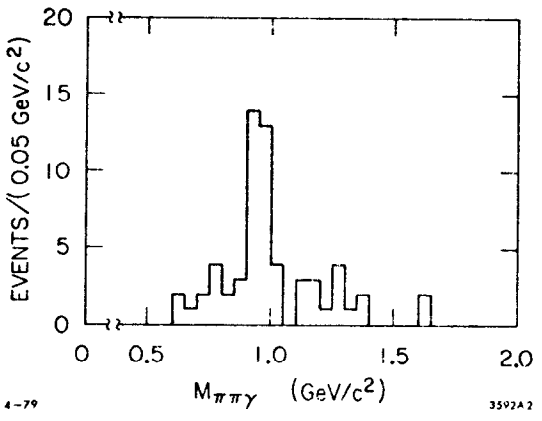

Fig. 11. $\pi^+\pi^-\gamma$ invariant mass distribution.

Their total energy peaks at low values thus excluding an interpretation of two-body production like $\eta'\gamma$ where the γ is undetected. The angular distribution is highly peaked in the forward and backward directions. We also observe a flat rapidity (y) distribution, shown in Figure 13, within the detector acceptance of about $-0.6 < y < 0.6$. These kinematical features are those expected for η' production by reaction (1) and are well reproduced by Monte Carlo generated two-photon events, using the two-photon calculation of Reference (15).

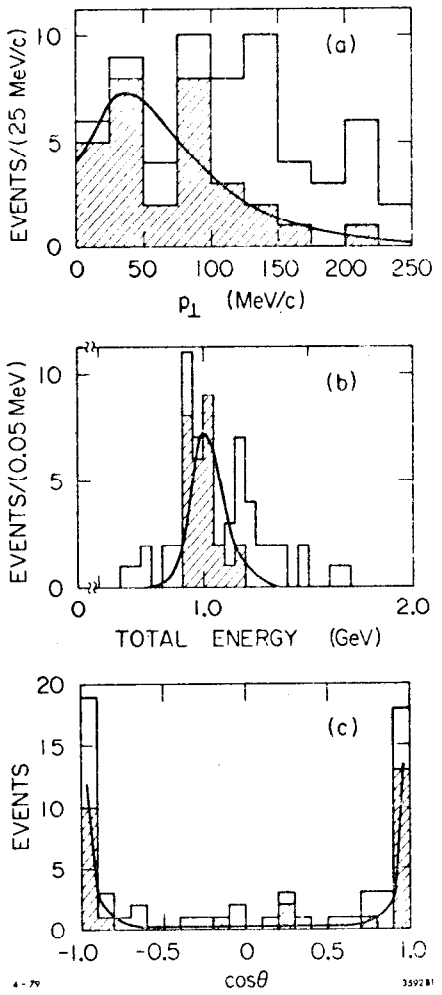

Fig. 12. Kinematical distributions for (a) transverse momentum, (b) total energy, and (c) cosine of the production angle with respect to the beam axis. The full histograms contain all events; the events in the η' mass peak are shaded. The curve represents the Monte Carlo calculation assuming $e^+e^- \to e^+e^-\eta'$ normalized to the observed η' signal.

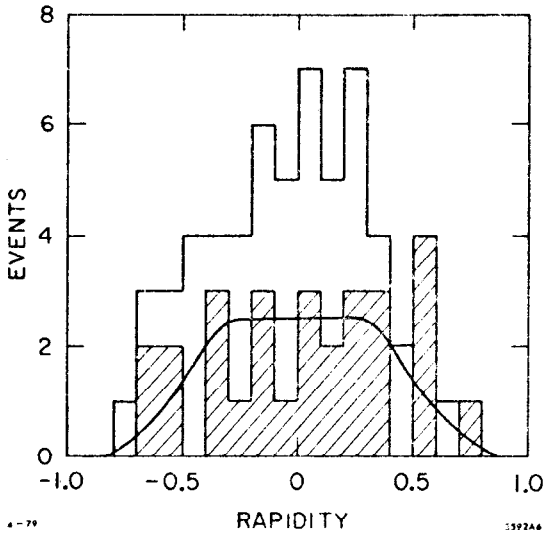

Fig. 13. Rapidity distribution for the $\pi^+\pi^-\gamma$ state. (Same definitions as for Figure 12).

The expected distributions, normalized to the same number of η' events, are shown as solid curves in Figures 12 and 13.

The background from e^+e^- annihilation events has been studied in multihadron events. The $\pi^+\pi^-\gamma$ mass combinations have been calculated independently of the existence of additional charged tracks or photons, with all other criteria unchanged. No peaking in the mass and energy distributions is seen, and the p_t distribution peaks above 200 MeV/c. The correction for annihilation events is included in the background subtraction using the adjacent mass regions which leaves a total of 23 ± 6 η' events (see Table 2).

The cross section for reaction (1) has been calculated using the branching ratio $B(\eta' \to \rho^0\gamma) = 0.298 \pm 0.017$ and is also given in Table 2. The cross section is directly proportional to the radiative width $\Gamma_{\gamma\gamma}(\eta')$.[16] Using the two-photon cross-section calculation of Reference (15), we determine $\Gamma_{\gamma\gamma}(\eta') = 5.9 \pm 1.6$ KeV.[17] The error is statistical only and does not include an estimated systematic uncertainty of ±20%. With the $B(\eta' \to \gamma\gamma) = 0.0197 \pm 0.0026$, the total width can then be determined to be $\Gamma_{tot}(\eta') = 300 \pm 90$ KeV (or $\tau = (2.2 \pm 0.7) \times 10^{-21}$ sec). Our measurement of Γ_{tot} is in excellent agreement with the only other available measurement (280 ± 100 KeV) recently reported by Reference (18).

There is considerable interest in a measurement of $\Gamma_{\gamma\gamma}(\eta')$.[19-21] Quark models with fractionally charged quarks and a small pseudoscalar octet-singlet mixing angle lead under the assumption of equal singlet and octet decay constants[20] to the prediction $\Gamma_{\gamma\gamma}(\eta') \simeq 6$ KeV.[19] This is in good agreement with our measurement. The data are also

Table 2. Summary of the Cross Section Calculation

E_b (GeV)	$\int \mathscr{L} dt$ (nb^{-1})	ε	$n_{\eta'}$	σ (nb)
2.21	798	0.017	5.1 ± 2.6	0.98 ± 0.50
2.25 - 2.50	2131	0.0224	4.3 ± 2.6	0.30 ± 0.18
2.50 - 3.00	1730	0.0217	10.3 ± 3.6	0.91 ± 0.32
3.70	984	0.0125	3.1 ± 2.2	0.84 ± 0.60

E_b is the beam energy, $\int \mathscr{L} dt$ the integrated luminosity, ε the detection efficiency [not including $B(\eta' \to \rho\gamma)$], $n_{\eta'}$ is the number of η' events (background subtracted) and σ is the observed cross section. Errors shown are statistical only.

in agreement with a recent relativistic quark model[21] calculation which predicts $\Gamma_{\gamma\gamma}(\eta') = 7.3$ KeV.

REFERENCES

1. W. Davies-White et al., Nucl. Instrum. Methods 160:227 (1979).
2. G. S. Abrams et al., IEEE Trans. on Nucl. Sci., NS-25:309 (1978).
3. R. L. Ford and W. R. Nelson, EGS Code, Stanford Linear Accelerator Center Report Number SLAC-210 (1978).
4. H. Brafman et al., IEEE Trans on Nucl. Sci. NS-25:1 (1978).
5. M. Piccolo et al., Phys. Rev. Lett. 39:1503 (1977).
6. R. Brandelik et al., Nucl. Phys. B148:189 (1979).
7. P. A. Rapidis et al., Phys. Rev. Lett. 39:526 (1977); W. Bacino et al., Phys. Rev. Lett. 40:671 (1978).
8. I. Peruzzi et al., Phys. Rev. Lett. 39:1301 (1977).
9. D. L. Scharre et al., Phys. Rev. Lett. 40:74 (1978).
10. S. J. Brodsky, T. Kinoshita and H. Terazawa, Phys. Rev. Lett. 25:972 (1970) and Phys. Rev. D4:1532 (1971); A. Jaccarini et al., Nuovo Cimento Lett. 4:933 (1970); N. Arteaga-Romera et al., Phys. Rev. D3:1569 (1971); V. N. Baier and V. S. Fadin, Nuovo Cimento Lett. 1:481 (1971).
11. V. E. Balakin et al., Phys. Lett. 34B:663 (1971); C. Bacci et al., Nuovo Cimento Lett. 3:709 (1972); G. Barbiellini et al., Phys. Rev. Lett. 32:385 (1974).

12. H. J. Besch et al., Phys. Lett. 81B:79 (1979).
13. S. Orito et al., Phys. Lett. 48B:380 (1974). L. Paoluzi et al., Nuovo Cimento Lett. 10:435 (1974).
14. G. S. Abrams et al, Stanford Linear Accelerator Center SLAC-PUB-2331 (1979)(submitted to Phys. Rev. Lett.).
15. V. M. Budnev and I. F. Ginzburg, Phys. Lett. 37B:320 (1971); V. N. Baier and V. S. Fadin, Nuovo Cimento Lett. 1:481 (1971), and private communication.
16. F. E. Low, Phys. Rev. 120:582 (1960).
17. Upper limins on $\Gamma_{\gamma\gamma}(\eta')$ have been published from two-photon experiments in References 12 and 13.
18. D. M. Binnie et al., Imperial College London preprint IC/HENP/79/2 (1979).
19. S. Okubo , in: "Symmetries and Quark Models," R. Chand, ed., Gordon and Breach, New York (1970); H. Suura, T. F. Walsh and B-L Young, Nuovo Cimento Lett. 4:505 (1972).
20. However, this assumption fails to describe $\Gamma(\eta' \to \pi^+\pi^-\gamma)/\Gamma(\eta' \to \gamma\gamma)$. See M. S. Chanowitz, Phys. Rev. Lett. 35:977 (1975) wherein an alternative analysis is proposed.
21. E. Etim and M. Greco, Nuovo Cimento 42:124 (1977).